PAPER www.rsc.org/materials | Journal of Materials Chemistry

Three-dimensional tetra(oligothienyl)silanes as donor material for organic solar cells

Sophie Roquet, Rémi de Bettignies, Philippe Leriche, Antonio Cravino and Jean Roncali*

Received 22nd March 2006, Accepted 16th May 2006
First published as an Advance Article on the web 9th June 2006
DOI: 10.1039/b604261a

Tetrahedral conjugated systems involving four conjugated oligothiophene chains fixed onto a central silicon node (**1**, **2**) have been synthesized and used as donor materials in hetero-junction solar cells. Bilayer solar cells have been realized by thermal evaporation of compounds **1** and **2** as donors and *N,N′*-bis-tridecylperylenedicarboxyimide as an acceptor. Comparison of the performances of these devices to those of a reference system based on dihexylterthienyl (H3T) shows that despite comparable effective conjugation lengths, the 3D compounds **1** and **2** lead to a power conversion efficiency four–five times higher, suggesting better absorption of the incident light and better hole transport properties. Whereas fabrication of bulk hetero-junction with H3T was prevented by the lack of film forming properties, a prototype bulk hetero-junction based on compound **2** as the donor and [6,6]-phenyl-C_{61}-butyric acid methyl ester (PCBM) as the acceptor has been realized. A short-circuit current density of 1.13 mA cm^{-2} and a power conversion efficiency of 0.30% has been measured under AM 1.5 simulated solar irradiation at 80 mW cm^{-2}.

Introduction

Thiophene-based linear π-conjugated oligomers and polymers are intensively investigated as active materials in organic field-effect transistors, (OFETs),[1] or solar cells.[2,3] Because of the specificity of charge-transport in these materials by inter-molecular charge-hopping and aromaticity transfer, achievement of high charge-carrier mobility requires a high degree of intermolecular order. The optimization of packing order in materials based on conjugated oligomers or polymers implies an increase of the crystallinity of the materials which is generally pursued through a precise control of the conditions of thermal evaporation for molecular materials[1,3,4] or by thermal post-treatment for polymer films.[2]

A consequence of the low dimensionality of organic semiconductors based on linear π-conjugated systems is the anisotropy of their charge-transport and optical properties which poses specific problems for devices fabrication. Thus, whereas a vertical orientation of the conjugated chains on the substrate improves mobility in organic field-effect transistors,[1,4] such an orientation is detrimental for solar cells as it strongly reduces the absorption of the incident light as well as charge transport to the electrodes.[3]

In an attempt to solve these problems, we have recently undertaken the development of three-dimensional conjugated architectures in order to reach new classes of organic semiconductors with isotropic charge-transport and optical properties.[5] Thus, we have shown that hybrid systems combining triphenylamine with oligothienylenevinylenes or oligothiophenes branches lead to interesting results for the fabrication of OFETs or heterojunction solar cells.[5]

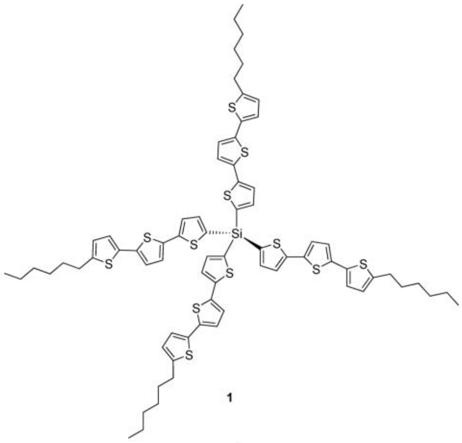

1

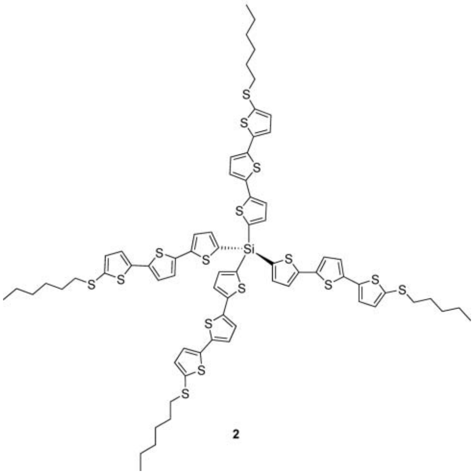

2

As a further step in the development of organic semiconductors based on 3D conjugated systems, we report here preliminary results on the use of tetrahedral molecules **1** and **2** as donor material in hetero-junction solar cells. These

---

Groupe Systèmes Conjugués Linéaires, CIMMA, UMR CNRS 6200, Université d'Angers, 2 Bd Lavoisier F-49045 Angers

compounds consist in four conjugated oligothiophene chains fixed onto a central silicon node. The four branches are end-capped with *n*-hexyl or hexylsulfanyl chains in order to increase the solubility of the final 3D system and to stabilize the cation radical by inductive and resonance effects[6] and by preventing follow-up chemical reaction during the process of hole-transport.

Results and discussion

The synthesis of the target compounds **1** and **2** is shown in Scheme 1. Friedel–Crafts acylation of terthiophene with hexanoic anhydride in the presence of tin chloride, followed by reduction of the obtained ketone by lithium aluminium hydride gave 2-hexyl-5,2′:5′,2″-terthiophene **3** in 80% overall yield. Reaction of bromohexane on thiophene-2-thiol **9** in the presence of tetrabutylammonium hydroxide gave 2-hexylsulfanylthiophene **8** in 85% yield. This compound was then converted into the corresponding stannyl derivative **7** by reaction with butyllithium and Bu_3SnCl. This Stille reagent was then coupled to 2-bromobithiophene (prepared by reaction of NBS on bithiophene) in the presence of a palladium catalyst to give terthienyl **6** in 72% yield. The target tetrahedral compounds were then prepared using the already reported procedure by treatment of terthienyls **3** and **6** with butyllitium at −78 °C followed by reaction with silicon tetrachloride.[7] Column chromatography on alumina gave compounds **1** and **2** in 34 and 59% yield respectively. However, all attempts to extend this approach to the synthesis of analog systems containing longer conjugated branches such as 2-hexylquaterthiophene remained unsuccessful due to the insufficient reactivity of the quaterthiophene anion. This implies that the future synthesis of analog systems containing longer conjugated branches should resort to a different synthetic approach.

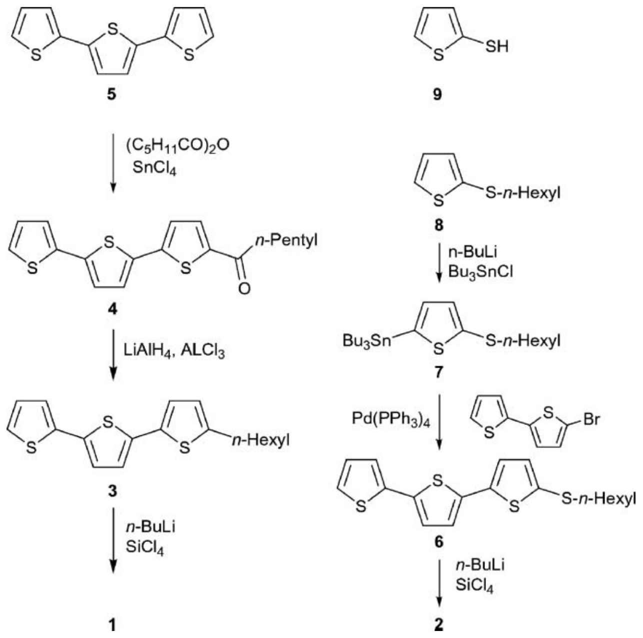

Scheme 1 Synthesis of the target compounds **1** and **2**.

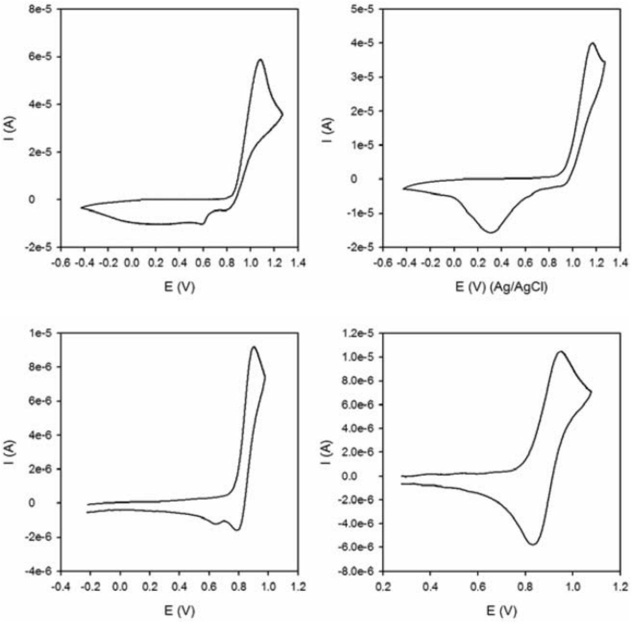

Fig. 1 Top: cyclic voltammograms of compounds **3** (left) and **1** (right); bottom: right **6** (left) and **2** (right) *ca.* 1 mmol L^{-1} in 0.10 M Bu_4NPF_6–CH_2Cl_2, scan rate 100 mV s^{-1}, ref. Ag.AgCl.

Fig. 1 shows the cyclic voltammograms of compounds **1** and **2** and of the reference linear compounds **3** and **6**. The CV of compounds **3** and **6** shows an irreversible anodic wave process at a peak potential (E_{pa}) of 1.10 and 0.90 V (Table 1). The less positive E_{pa} value of compound **6** reflects the stronger electron-releasing effect of the alkylsufanyl group compared to the hexyl chain. The weak cathodic peak observed at 0.60 V in the reverse scan suggests a dimerization of the cation radical to produce the corresponding sexithiophene. The CV of the tetrahedral compounds **1** shows an irreversible anodic peak at 1.15 V. The slight increase of E_{pa} compared to the linear compound **3** can be attributed to a lower diffusion coefficient of the tetrahedral compound **1**.[8] The CV of compound **1** shows a broad cathodic wave in which a weak peak is still discernible at 0.60 V. This behaviour suggests that the cation radical of compound **1** is not stable but undergoes a follow-up reaction with a break of the carbon–silicon bond and formation of a dimerization product. In fact, it has been shown already that thiophenes and oligothiophenes bearing silyl group at the terminal α-positions can be readily electropolymerized.[9]

As shown by the CV of compound **2**, the introduction of the sulfide group in the substituent leads to a fully reversible oxidation process with E_{pa} at 0.94 V indicating a stable cation radical. Compared to compound **1**, this stabilization can be

Table 1 Cyclic voltammetric data (in the conditions of Fig. 1), and optical data in CH_2Cl_2 for compounds **1**, **2** and the corresponding branches **3** and **6**

Compd	E_{pa}/V	λ_{max}/nm
3	1.10	367
1	1.15	384
6	0.90	371
2	0.94	390

attributed to the stronger electron-releasing effect of the alkylsufanyl group.

UV–vis. absorption data recorded in solution show that for both linear and 3D compounds, replacement of hexyl substituents by hexylsulfanyl ones produces a slight red shift of λ_{max}. Comparison of the λ_{max} of the 3D systems to those of the corresponding linear chain reveals a red shift of 17 and 19 nm for compounds **1** and **2** respectively. This phenomenon can be attributed to the inductive effect of the silane substituent. Fig. 2 shows the UV–vis. spectra of compounds **1** and **2** in methylene chloride solution and as a thin film on glass prepared by thermal evaporation under vacuum. The spectrum of the film of compound **1** shows a red shift of λ_{max} from 384 to 406 nm and the development of a fine structure with a second maximum at 427 nm. This phenomenon can be attributed to intermolecular interactions between the conjugated branches in the solid state. Surprisingly, this effect is not observed for compound **2** for which the spectrum of the film is practically identical to the solution spectrum except for a slight broadening of the absorption band.

This different behaviour suggests that the sulfide groups in the substituents do not allow tight interactions between the conjugated branches in the solid. Further work and in particular X-ray analysis is needed to clarify this point. The spectra of the two films present an absorption onset at around 470 nm which correspond to a band gap of ~2.65 eV.

Compounds **1** and **2** have been used as the donor material in bilayer hetero-junction solar cells with *N,N′*-bis-tridecyl-perylenedicarboxyimide (DP13) as the acceptor and electron transport layer. Cells of 6 mm diameter have been realized on ITO substrates spin-coated with a 30 nm film of Baytron P®. The donor and acceptor layers were deposited successively by thermal evaporation under vacuum and the devices were completed by deposition of a 5 Å thick layer of LiF and of an 80 nm thick aluminium electrode.

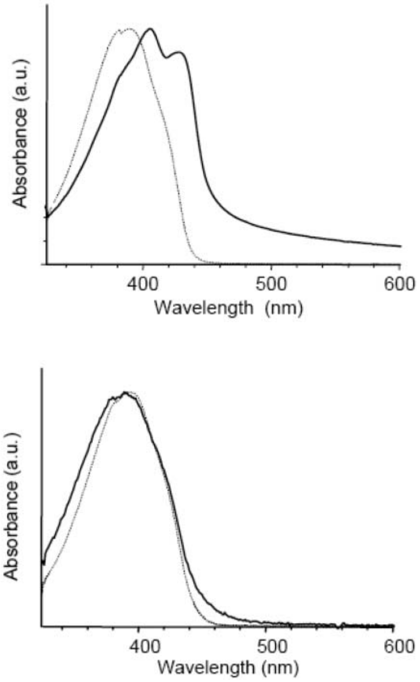

Fig. 2 Normalized UV–vis absorption spectra of compound **1** (top) and **2** (bottom). Dotted line: in CH_2Cl_2, solid line: thin films prepared by thermal evaporation on glass.

Fig. 3 shows the UV–vis. absorption and photo-current action spectra of the cells based on compounds **1** and **2** under monochromatic irradiation. The absorption spectra show that the cell based on **1** presents a much higher absorbance in the 400 nm region. While the smaller thickness of the film of **2** (16 nm instead of 20 nm for **1**) can account for part of this difference, other factors probably play a major role such as molecular packing in the solid state and interactions of the molecules with the Baytron® treated ITO surface. Another possible origin for this phenomenon could involve partial re-sublimation of the film of compound **2** during the thermal evaporation of the acceptor layer due to the relatively low melting point of donor **2** (132 °C). Further work is needed to clarify this point.

The action spectrum of the cell based on compound **1** shows a first broad maximum of the external quantum efficiency (EQE) of *ca.* 18% at 400 nm corresponding to the absorption band of the donor **1** followed by a tail extending to 650 nm corresponding to the absorption region of DP13. The EQE spectrum of the cell based on compound **2** shows a maximum EQE of 12% at 400 nm followed by shoulders of 8% and 5% around 480 and 580 nm corresponding to the absorption features of DP13. The higher EQE observed at these wavelengths compared to the cell based on **1** is probably the consequence of the lower absorbance of the film of **2** which allows a direct photo-excitation of the DP13 layer.

Fig. 4 shows the current-density voltage curves of the two cells in the dark and under simulated AM 1.5 solar irradiation at 80 mW cm^{-2} power intensity. The curves recorded in the dark show a rectification behaviour with a current onset at 0.90 and 0.60 V for the cells based on donor **1** and **2** respectively.

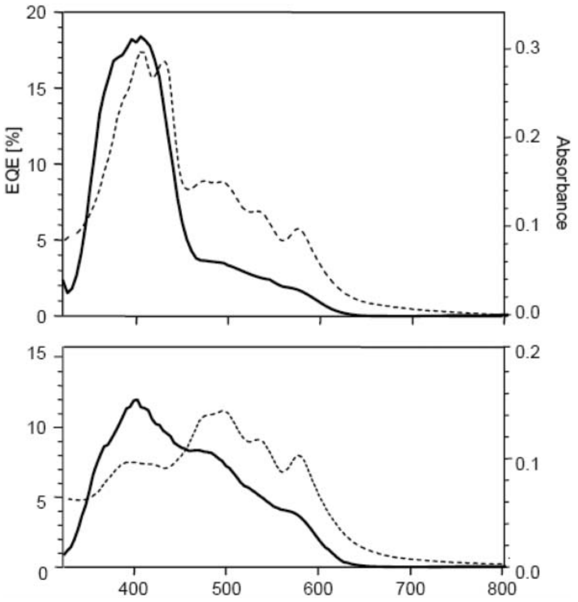

Fig. 3 Photo-current action spectra of the hetero-junction solar cells. Top: donor **1** (20 nm) and DP13 (20 nm), bottom donor **2** (16 nm) and DP 13 20 nm. The dotted lines correspond to the optical spectra of the bilayer.

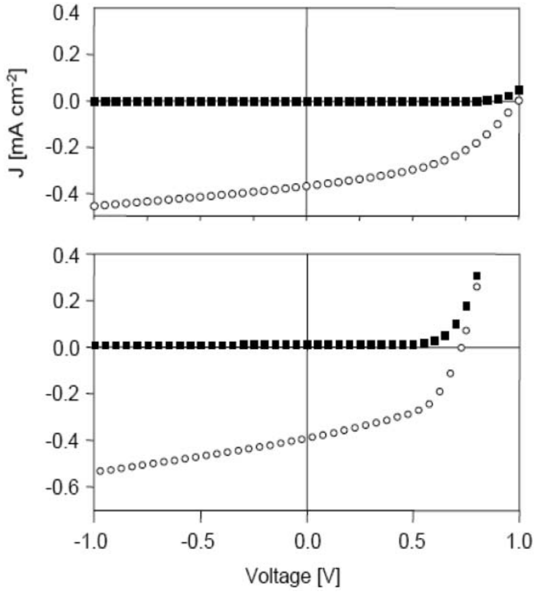

Fig. 4 Current density curves of the bilayer cells based on donor **1** (top) and **2** (bottom) in the dark (■) and under white light irradiation at 80 mW cm^{-2} light intensity (○).

Under irradiation the cells deliver short-circuit current densities (J_{sc}) of 0.36 and 0.44 mA cm^{-2} respectively and open-circuit voltage (V_{oc}) of 0.99 and 0.74 V. The V_{oc} values which are tightly correlated with the oxidation potentials of the two donors confirm the major influence of the oxidation potential of the donor on V_{oc}.[10] Combined with filling factors (*FF*) of 0.45 and 0.49 these data lead to power conversion efficiencies of 0.20 and 0.17% for the cells based on donor **1** and **2** respectively (Table 2).

A reference cell realized using dihexylterthienyl (H3T) as the donor gave the following results: J_{sc} = 0.14 mA cm^{-2}, V_{oc} = 0.76 V and *FF* = 0.32. Comparison of these results to those obtained with the tetrahedral systems **1** and **2** clearly show that the 3D donors **1** and **2** lead to much better results. Since dihexylterthienyl and the 3D compounds **1** and **2** have comparable absorption spectra, the better results obtained with the 3D donors can be attributed to the combined effect of a better absorption of the incident light and better hole transport (as suggested by the better *FF* values). Since thermally evaporated dialkyl-oligothiophenes are known to orient vertically on surface such an orientation limits both the absorption of the incident light and hole transport through the cell thickness.[1,3,4]

Based on a larger solubility of compound **2** due among other things, to weaker interactions in the solid state, a first evaluation of the potentialities of this compound as donor in bulk hetero-junctions solar cells has been carried out. To this end, a prototype cell has been realized by spin-casting a composite film of donor **2** and [6,6]-phenyl-C_{61}-butyric acid methyl ester (PCBM) as the acceptor in a 1 : 3 ratio. A mixture of a donor **2** and PCBM dissolved in *o*-dichlorobenzene was spun cast on a Baytron modified ITO electrode and the device was completed by evaporation of a 80 nm thick aluminium electrode.

Table 2 Photovoltaic characteristics of the bilayer[a] and bulk[b] hetero-junctions based on donor **1** and **2** under while light irradiation at 80 mW cm^{-2}

Device	V_{oc}/V	J_{sc}/mA cm^{-2}	*FF*	η(%)
H3T-DP13	0.76	0.14	0.32	0.04
1-DP13[a]	0.99	0.36	0.46	0.20
2- DP13[a]	0.76	0.37	0.49	0.17
2/PCBM[b]	0.85	1.13	0.24	0.29

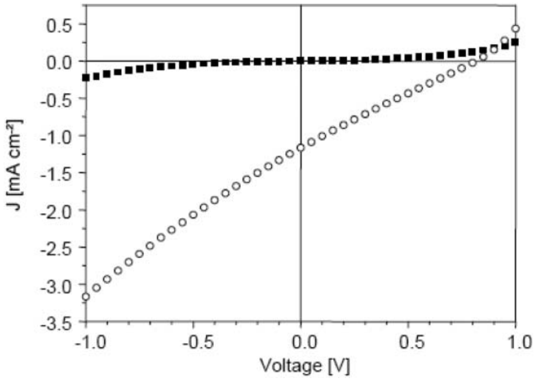

Fig. 5 Current density curves of a bulk hetero-junction based on donor **2** and PCBM (ratio 1 : 3) in the dark (■) and under white light irradiation at 80 mW cm^{-2} light intensity (○).

Fig. 5 shows the current-density–voltage curves of the cell. In the dark the *J–V* curve is symmetrical indicating an absence of rectification. The curve recorded under white light illumination shows an increasing slope at negative voltage which may reflect either important charge recombination or current leakage. Under white light irradiation the cell delivers a J_{sc} of 1.13 mA cm^{-2} and V_{oc} of 0.85 V. With a low *FF* value of 0.24 these data lead to a power conversion efficiency of 0.29%. An attempt to realize a reference cell with H3T failed because of the lack of film forming properties of this compound.

Conclusion

Tetrahedral conjugated systems have been synthesized by grafting terthienyl chains end capped with hexyl and hexylsulfanyl chains on a silicon node. Electrochemical and UV–vis results underline the major role of the end-substituents on the stability of the cation-radical and on the intermolecular interactions in the solid state.

A preliminary evaluation of the potentialities of these 3D conjugated systems as donor material in organic solar cells has been carried out. The results obtained with bilayer and bulk hetero-junction solar cells show that compared to a reference 1D terthienyl donor, the 3D architecture leads to a significant improvement of the cells' performances attributed to the isotropic absorption and hole transport associated with the 3D geometry.

Although the cell performances are drastically limited by the poor absorption of the visible light by the donors, the first results obtained with these short chain model compounds confirm the interest of the 3D approach and they provide a strong incitement to synthesize other 3D conjugated systems with longer effective conjugation length and hence extended absorption in the visible spectral region. Work in these directions is now underway and will be reported in future publications.

Experimental

5-hexanoyl-2, 2′:5′, 2″-terthiophene

To a solution of terthiophene (4.5 g, 16 mmol) and hexanoic anhydride (4.23 mL, 1.1 eq.) in anhydrous methylene chloride are added dropwise 2.08 mL (1.1 eq.) of tin tetrachloride. The dark red solution is stirred at room temperature for 5 h. The mixture is poured onto a mixture of ice and acetic acid, methylene chloride is added and the organic phase is washed with 10% aqueous NaOH and water and dried over $MgSO_4$. Solvent evaporation and column chromatography (silica gel, 1 : 1 petroleum ether/methylene chloride, leads to 3.64 g (66%) of a brown solid. M.p. 133 °C

5-hexyl-2, 2′:5′,2″-terthiophene

A mixture of 5-hexanoylterthiophene (3.61 g, 10.4 mmol), aluminium trichloride (2.76 g) and $LiAlH_4$ (3.15 g, 8 eq) in 100 mL of anhydrous ether is stirred under inert atmosphere at ambient temperature for 3 h 30 min. Ethyl acetate (25 mL) and 6 M aqueous HCl (30 mL) are added and the solution is stirred for 1 h 30 min. After addition of water, the aqueous phase is extracted with ether, the organic phase is washed with saturated aqueous Na_2CO_3 and water and dried over $MgSO_4$. Solvent evaporation and column chromatography (silica gel, petroleum ether) gave 2.78 g (80%) of a yellow solid. Mp 66 °C. ^{1}H NMR ($CDCl_3$) 7.20 (dd, 1H, ^3J = 5.10Hz; ^4J = 1.10Hz), 7.15 (dd, 1H, ^3J = 3.60Hz, ^4J = 1.10Hz), 7.05 (d, 1H, ^3J = 3.80Hz), 7.01 (dd, 1H, ^3J = 5.10Hz, ^3J = 3.60Hz), 6.99 (d, 1H, ^3J = 3.80Hz), 6.98 (d, 1H, ^3J = 3.50Hz), 6.68 (d, 1H, ^3J = 3.50Hz), 2.79 (t, 2H, ^3J = 7.70Hz), 1.38 (quint, 2H, ^3J = 7.60Hz), 1.31 (m, 6H), 0.89 (t, 3H, ^3J = 6.90Hz, CH_3).

5-hexylsulfanyl-2, 2′:5′, 2″-terthiophene

A mixture of 5-bromo-2,2′-bithiophene, (2.5 g, 10 mmol), 5-hexylsulfanyl-2-tributylstanniothiophene (12.41 g, 1 eq.), and $Pd(PPh_3)_4$, (1.46 g 5 mol%) and 250 mL of toluene is refluxed under nitrogen for 17 h. After return to room temperature the residue is dissolved in 100 mL of dichloromethane. The organic phase is washed with water and dried over $MgSO_4$. Solvent evaporation and column chromatography (silica gel, petroleum ether) gave 2.64 g (72%) of a yellow solid. M.p. 60 °C, ^{1}H NMR ($CDCl_3$) 7.22 (dd, 1H, ^3J = 5.08Hz, ^4J = 1.02Hz), 7.17 (dd, 1H, ^3J = 3.61Hz, ^4J = 1.05Hz), 7.07 (d, 1H, ^3J = 3.72Hz), 7.04 (d, 1H, ^3J = 3.78Hz), 7.02 (dd, 1H, ^3J = 5.05Hz, ^3J = 3.67Hz), 7.02 (d, 1H, ^3J = 4.09Hz), 7.00 (d, 1H, ^3J = 3.69Hz), 2.81 (t, 2H, ^3J = 7.32Hz), 1.64 (quint, 2H, ^3J = 7.50Hz), 1.41 (m, 2H), 1.29 (m, 4H), 0.87 (m, 3H).

Tetrakis(5″-hexyl-5-terthienyl)silane (1)

To a solution of 5-hexyl-2,2′:5′,2″-terthiophene (2 g) in 30 mL of dry ether is added dropwise 3.6 mL (0.97 eq.) of butyllithium (1.6 M in hexanes). The solution is stirred for 30 min at 0 °C then 2 h at room temperature. Silicon tetrachloride (0.11 mL, 0.17 eq.) in 10 mL of dry ether is added at 0 °C. The mixture is stirred for 10 min at 0 °C and overnight at room temperature. After addition of 450 mL of dichloromethane the organic phase is washed with water and dried over $MgSO_4$. Solvent evaporation and column chromatography (alumina, 5 : 1 petroleum ether/methylene chloride) gave 0.86 g (59%) of a yellow solid. M.p. 160 °C. ^{1}H NMR ($CDCl_3$) 7.43 (d, 1H, ^3J = 3.58Hz), 7.29 (d, 1H, ^3J = 3.57Hz), 7.13 (d, 1H, ^3J = 3.82Hz), 6.99 (d, 1H, ^3J = 3.78Hz), 6.98 (d, 1H, ^3J = 3.58Hz), 6.68 (d, 1H, ^3J = 3.57Hz), 2.79 (t, 2H, ^3J = 7.55Hz), 1.66 (quint, 2H, ^3J = 7.52Hz), 1.36 (m, 2H), 1.30 (m, 4H), 0.87 (m, 3H). ^{13}C NMR ($CDCl_3$): 145.8, 145.4, 139.4, 137.6, 134.8, 134.3, 131.4, 125.2, 124.9, 124.9, 123.6, 123.5, 31.5, 31.5, 30.2, 28.7, 22.6, 14.1. MS MALDI-TOF calcd for $C_{72}H_{76}S_{12}Si$ 1352, found 1353 $(M + H)^+$.

Tetrakis(5″-hexylsulfanyl-5-terthienyl)silane (2)

To a solution of 1 g of 5-hexylsulfanyl-2,2′:5′,2″-terthiophene in 15 mL of dry ether is added dropwise at −78 °C, 1.7 mL, (0.97 eq.) of butyllithium 1.6 M in hexanes. The solution is stirred for 30 min at 0 °C then 2 h at room temperature. Silicon tetrachloride (0.05 mL, 0.17 eq.) in 5 mL of dry ether is added at 0 °C. The mixture is stirred 10 min at 0 °C and 4 h at room temperature. After addition of 60 mL of dichloromethane the organic phase is washed with water and with a saturated aqueous NaCl and dried over $MgSO_4$. Solvent evaporation and column chromatography (alumina, 4 : 1 petroleum ether/methylene chloride) gave 0.23 g (34%) of a yellow solid. Mp 132 °C. ^{1}H NMR ($CDCl_3$): 7.43 (d, 1H, ^3J = 3.58Hz), 7.31 (d, 1H, ^3J = 3.57Hz), 7.14 (d, 1H, ^3J = 3.86Hz), 7.04 (d, 1H, ^3J = 3.77Hz), 7.02 (d, 1H, ^3J = 3.67Hz), 6.99 (d, 1H, ^3J = 3.79Hz), 2.81 (t, 2H, ^3J = 7.37Hz), 1.62 (quint, 2H, ^3J = 7.50Hz), 1.40 (quint, 2H, ^3J = 7.53Hz), 1,30 (m, 4HH), 0.88 (t, 3H, ^3J = 6.91Hz). ^{13}C NMR ($CDCl_3$): 145.1, 139.8, 139.4, 136.6, 135.6, 134.6, 133.9, 131.6, 125.2, 125.1, 124.4, 123.8, 38.9, 31.3, 29.3, 28.1, 22.5, 13.9. M.S. MALDI-TOF SM calcd for $C_{72}H_{76}S_{16}Si$ 1480 found 1481 $(M + H)^+$ 1480. Anal (calcd) C 58.84 (58.33) H 5.54 (5.17) Si 1.87 (1.89).

Fullerene C_{60} (99+%) was purchased from Merck and used without further purification. The indium–tin–oxide (ITO) coated glass substrates (Solems) with a sheet resistance of 40 ohm square^{-1} were cleaned in an ultrasonic bath with aqueous detergent, ethanol and acetone dried in an oven and treated 15 min with an UV–ozone cleaner (Jelight 42–220, 28 W cm^{-2}). ITO substrates were then spin-coated with a 60 nm film of poly(3,4-ethylenedioxythiophene)-poly(styrene-sulfonate) (Baytron P®) and dried at 115 °C for 15 min. Layers of compound **1** and C_{60} were thermally evaporated in a Plassys ME300 chamber at a pressure of about 10^{-6} mbar and at rate of ~1.5 Å s^{-1}. A glass slide placed near the ITO substrates was used to obtain samples for UV–vis absorption spectra. The device were completed by the evaporation of aluminium films (*ca.* 60 nm thick) as negative electrodes. A shadow mask with openings of 6 mm diameter was used to define a device's area of 0.30 cm^2. After their fabrication, the devices were stored and characterised in a glove-box (200B, MBraun). The J–V curves were recorded in the dark and under various light intensities using a Keithley 236 source-measure unit and a home-made acquisition program.

Power conversion efficiencies were measured with a Steuernagel Solar constant 575 simulator. Light intensity was measured with a calibrated broadband optical power meter (Melles Griot) and was varied with neutral density filters.

The devices were illuminated through the ITO electrode side. The efficiency values were neither corrected for a possible spectral mismatch of the light source with the solar spectrum nor for the absorption/reflection losses at the various interfaces.

EQE was measured with a Perkin Elmer 7225 lock-in amplifier under monochromatic illumination at variable wavelength at a chopping frequency of 100 Hz. The light source was a tungsten lamp (Acton SpectraPro150).

Absorption spectra were recorded with a Perkin Elmer Lambda 19 UV–visible–Near IR spectrophotometer. Cyclic voltammetry was performed in a three electrode cell with an EGG 273 potentiostat.

References

1 C. D. Dimitrakopolous and P. Malenfant, *Adv. Mater.*, 2002, **14**, 99.

2 (*a*) C. J. Brabec, N. S. Sariciftci and J. C. Hummelen, *Adv. Funct. Mater.*, 2001, **11**, 15; (*b*) W. Ma, C. Yang, X. Gong, K. Lee and A. J. Heeger, *Adv. Funct. Mater.*, 2005, **15**, 1617; (*c*) T. Erb, U. Zhokhavets, G. Gobsch, S. Raleva, B. Stühn, P. Schilinsky, C. Waldauf and C. J. Brabec, *Adv. Funct. Mater.*, 2005, **15**, 1193; (*d*) G. Li, V. Schrotriya, J. Huang, Y. Yao, T. Moriarty, K. Emery and Y. Yang, *Nat. Mater.*, 2005, **4**, 864; (*e*) N. Camaioni, G. Ridolfi, G. Casalbore-Miceli, G. Possamai and M. Maggini, *Adv. Mater.*, 2002, **14**, 1735.

3 (*a*) C. Videlot, A. El Kassmi and D. Fichou, *Sol. Energy Mater. Sol. Cells*, 2000, **63**, 69; (*b*) R. de Bettignies, Y. Nicolas, P. Blanchard, E. Levillain, J.-M. Nunzi and J. Roncali, *Adv. Mater.*, 2003, **15**, 1939.

4 (*a*) F. Garnier, A. Yassar, R. Hajlaoui, G. Horowitz, F. Deloffre, B. Servet, S. Ries and P. Alnot, *J. Am. Chem. Soc.*, 1993, **115**, 8716; (*b*) H. E. Katz, A. J. Lovinger and J. G. Laquindanum, *Chem. Mater.*, 1998, **10**, 457; (*c*) C. Videlot, J. Ackermann, P. Blanchard, J.-M. Raimundo, P. Frère, M. Allain, R. de Bettignies, E. Levillain and J. Roncali, *Adv. Mater.*, 2003, **15**, 306.

5 (*a*) A. Cravino, S. Roquet, P. Leriche, O. Alévêque, P. Frère and J. Roncali, *Chem. Commun.*, 2006, 1416; (*b*) S. Roquet, A. Cravino, P. Leriche, O. Alévêque, P. Frère and J. Roncali, *J. Am. Chem. Soc.*, 2006, **128**, 3459; (*c*) A. Cravino, S. Roquet, O. Alévêque, P. Leriche, P. Frère and J. Roncali, *Chem. Mater.*, 2006, **18**, 2584.

6 R. G. Hicks and M. B. Nodwell, *J. Am. Chem. Soc.*, 2000, **122**, 6746.

7 J. Roncali, C. Thobie-Gautier, H. Brisset, J. F. Favard and A. Guy, *J. Electroanal. Chem.*, 1995, **381**, 257.

8 A. J. Bard and L. R. Faulkner, *Electrochemical Methods. Fundamentals and Applications*, Wiley, New York, 1980.

9 (*a*) M. Lemaire, W. Büchner, A. Guy, R. Garreau and J. Roncali, *J. Electroanal. Chem.*, 1990, **281**, 293; (*b*) J. Roncali, A. Guy, M. Lemaire, R. Garreau and H. A. Hoa, *J. Electroanal. Chem.*, 1991, **312**, 277.

10 A. Gadisa, M. Svensson, M. R. Andersson and O. Inganäs, *Appl. Phys. Lett.*, 2004, **84**, 1609.